Three dimensionally confined optical modes in quantum-well microtube ring resonators

Ch. Strelow, C. M. Schultz, H. Rehberg, H. Welsch, Ch. Heyn, D. Heitmann, and T. Kipp*
Institut für Angewandte Physik und Zentrum für Mikrostrukturforschung, Universität Hamburg, Jungiusstraße 11, 20355 Hamburg, Germany

(Received 15 February 2007; revised manuscript received 2 May 2007; published 5 July 2007)

We report on microtube ring resonators with quantum wells embedded as an optically active material. Optical modes are observed over a broad energy range. Their properties strongly depend on the exact geometry of the microtube along its axis. In particular, we observe (i) preferential emission of light on the inside edge of the microtube and (ii) confinement of light also in the direction of the tube axis by an axially varying geometry, which is explained in an expanded waveguide model.

DOI: 10.1103/PhysRevB.76.045303 PACS number(s): 78.66.Fd, 78.67.De, 42.82.Cr, 42.55.Sa

Semiconductor microcavities confining light on the scale of its wavelength have gained considerable interest in the past years, both for possible applications in integrated optoelectronics and for basic research on light-matter interaction, the latter especially in cavity quantum electrodynamic experiments.[1,2] Another growing field in the past years is the research on semiconductor micro- and nanostructures fabricated by use of strain relaxation of pseudomorphically grown bilayers, which are lifted off the substrate.[3–8]

We have recently shown that, by combining both research fields, it is possible to fabricate rolled-up microtubes which act as optical ring resonators.[7] In this paper, we report on a microtube ring resonator design with embedded quantum wells (QWs) as optically active material instead of self-assembled quantum dots as in our previous work. We observe optical modes over a broad energy range expanding from a little above the QW center emission energy to its low-energy side. The quality factor of the modes and its mode spacing are affected by reabsorption of light by the QW. We study the mode structure of our microtubes by scanning photoluminescence spectroscopy along the tube axis. The interesting aspect of our investigation is that we clearly observe (i) preferential emission of light at the axial edges and (ii) confinement of optical modes also along the tube axis. The latter is caused by spatially varying revolution numbers. Taking into account the exact geometric dimensions which we derive from scanning electron microscope (SEM) investigations, the spatial dependency of the mode energies along the tube axis can be nicely calculated.

The starting point of the fabrication of our QW microtube ring resonator is a molecular beam epitaxy grown layer system. On a GaAs substrate and a GaAs buffer layer, 40 nm AlAs will serve as a sacrificial layer in the later processing. The strained layer system which will by lifted off the substrate consists of 14 nm $In_{0.15}Al_{0.21}Ga_{0.64}As$, 6 nm $In_{0.19}Ga_{0.81}As$, 41 nm $Al_{0.24}Ga_{0.76}As$, and 4 nm GaAs. Both In-containing layers are pseudomorphically strained grown. The InGaAs layer forms a QW sandwiched between higher band gap barriers. The actual preparation process of self-supporting microtube bridges by using optical lithography and wet etching processes starts with the definition of a U-shaped strained mesa followed by the definition of a starting edge. The details can be found in Ref. 7. Here, we further improved our preparation technique by etching deeply into the AlAs layer in the region between the legs of the U-shaped mesa (see SEM picture in Fig. 1). During the following selective etching step, this region is protected by photoresist. This process leads to a larger and more controllable lifting of the central part of the microtube from the substrate. The SEM image in Fig. 1 depicts the specific microtube on which all measurements presented in this paper have been performed. It is slightly more than twofold rolled in its self-supporting part; correspondingly, the wall thickness is mostly 130 nm except for the small region along the tube axis where three strained sheets sum up to a 195 nm thick wall. The self-supporting part has a diameter of about 6.4 μm and a distance to the substrate of about 1 μm. The left inset in Fig. 1 sketches a *nonscaled* cross section of the microtube.

We investigated our microtubes by microphotoluminescence spectroscopy at low temperature $T=7$ K. A He-Ne laser ($\lambda=633$ nm) was focused on the sample by a microscope objective ($50\times$), having a spot diameter of about 1.5 μm.

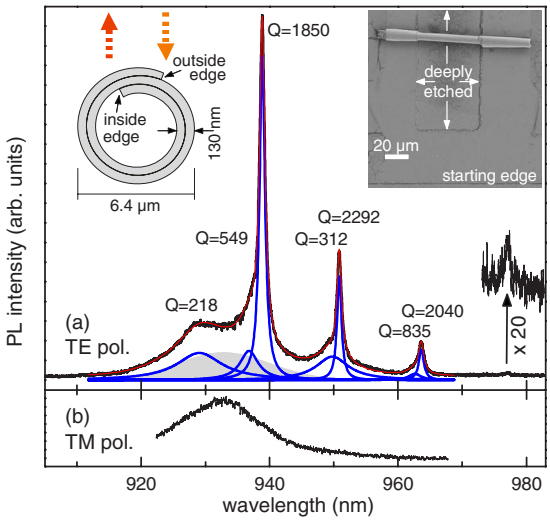

FIG. 1. (Color online) Measured PL spectra (black lines) of the microtube for (a) TE and (b) TM polarizations. The excitation power density was about 4 kW/cm^2. The spectrum in (a) is approximated by the sum of Lorentzian curves for the resonant modes (below the measured spectrum) and a Gaussian curve for the leaky modes (gray shaded). Q factors have been obtained by fitting. The left inset shows a nonscaled cross-sectional sketch of the microtube together with the excitation and collection configuration; the right inset shows a SEM image of the microtube.

The PL light was collected by the same objective, dispersed by a 1 m monochromator and detected by a cooled charge coupled device (CCD) camera.

Figure 1(a) shows a photoluminescence (PL) spectrum of the microtube. The sequence of sharp peaks represents optical modes which are observed here in microtubes containing QWs. Before discussing these modes in more detail, we want to point out the excitation and collection configuration used in this measurement. Here, the positions of excitation and collection of the PL light were the same in the z direction along the microtube axis but could be shifted against each other in the radial direction of the microtube. This situation is illustrated in the schematic inset in Fig. 1 by the two vertical arrows. The exciting laser generates electrons and holes which quickly relax into the QW in the vicinity of the focused laser spot on the microtube. There they form excitons which then radiatively decay. A fraction of the emitted light does not fulfill the condition of total reflection on the tube-wall–air interface and therefore couples to leaky modes. The other fraction does fulfill the condition of total reflection and is therefore guided by the tube wall. Constructive interference leads to the formation of optical resonator modes when, in a rather simple picture, light guided perpendicularly to the tube axis has the same phase after one round trip. Therefore, collecting the light at a different position than exciting the QW suppresses the detection of light out of leaky modes with respect to the cavity mode emission. If we collect the PL light from the excitation position, we can identify the emission into leaky modes around 933 nm with a full width at half maximum (FWHM) of 14 nm (23 meV). This is explicitly shown in Fig. 3(d), which will be discussed later in the text. This signal is not affected by interference inside the ring resonator and represents the emission of a curved QW. It is redshifted by about 20 nm (30 meV) compared to the QW emission of the unstructured sample, which is shown in Fig. 2(a). The shifting is strain induced and has been similarly reported by Hosoda *et al.*[5]

We now want to discuss the resonator modes in more detail. All modes are linearly polarized with the electric field vector parallel to the tube axis [TE polarization, Fig. 1(a)]. We find no modes in perpendicular polarization, as can be seen in Fig. 1(b). The strong peaks at about 939, 951, and 963.5 nm clearly show shoulders on their high-energy side. Their origin is not unambiguously clear. They might arise due to the lifting of the degeneracy of a perfectly symmetric cylindrical resonator by the inner and outer edges of the real structure (see sketch in Fig. 1).[9] Another explanation for the double peak structure might be the existence of axially confined modes of slightly different energy, which spatially overlap or at least cannot be separated by our experimental setup. Such axially localized modes will be thoroughly addressed later in this paper. At about 977 nm, a further mode with low intensity can be seen [marked by an arrow and magnified by a factor of 20 in Fig. 1(a)]. By trying to approximate the spectrum by a superposition of Lorentzians for the resonant modes and their high-energy shoulders together with a homogeneous Gaussian curve at about 933 nm with its above given FWHM for the residual intensity from leaky modes, one can clearly identify a further, rather broad mode on the high-energy side of the QW emission at about 929 nm. This peak can clearly be observed only in the described excitation and detection configuration. Collecting the PL light at the excitation position would strongly overlay this peak by leaky modes.

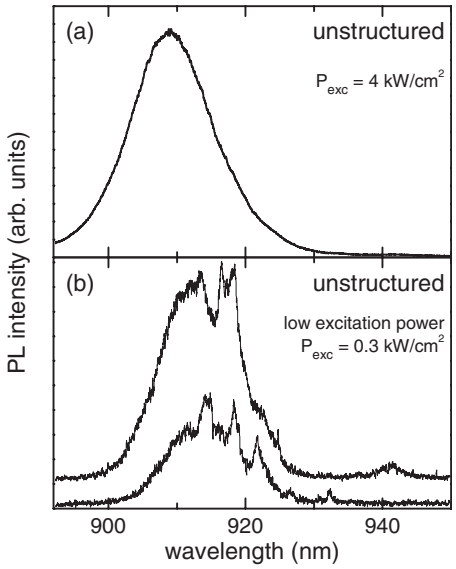

FIG. 2. PL spectra of the unstructured sample obtained with different excitation power densities: (a) 4 kW/cm^2 and (b) 0.3 kW/cm^2. The spectra in (b) (vertically shifted for clarity) were obtained in one and the same measurement for slightly different spatial positions within the area of the laser spot.

Recapitulating, altogether, five linearly polarized optical modes plus some shoulders are observed over an energy range of about 50 nm (70 meV). These modes are reported here in microtube ring resonators containing QWs as the optically active material. The lowest lying mode is separated by about 44 nm (60 meV) from the center QW emission energy. The observation of similar low lying cavity modes has been reported for microdisks containing ternary AlGaAs QWs, and they were attributed to the recombination of electron-hole pairs localized in monolayer and alloy fluctuations.[10] In fact, in measurements with low excitation power density on our unstructured sample, we observe single sharp lines with spatially changing energy positions on the low-energy side of the QW emission, as expected for emission out of such localized states. This can be seen in Fig. 2(b) where the excitation power was decreased by more than a factor of 10 compared to the measurements shown in Fig. 2(a) or in Fig. 1. Both spectra were obtained in one and the same measurement for slightly different spatial positions within the area of the laser spot. Regarding the quality factors $Q=E/\Delta E$, one can deduce a weak trend of slightly decreasing Q factors for increasing mode energies, still below the center QW emission energy if one averages the values of the main modes and its corresponding neighbors. This weak decreasing can be explained with a slight increase of reabsorption of light inside the cavity. Absorption is strongly enhanced for energies above the QW emission center. Consequently, the optical mode above the QW emission energy experiences strong losses resulting in a broadening by a factor of about 10 compared to the sharpest peaks on the low-energy side.

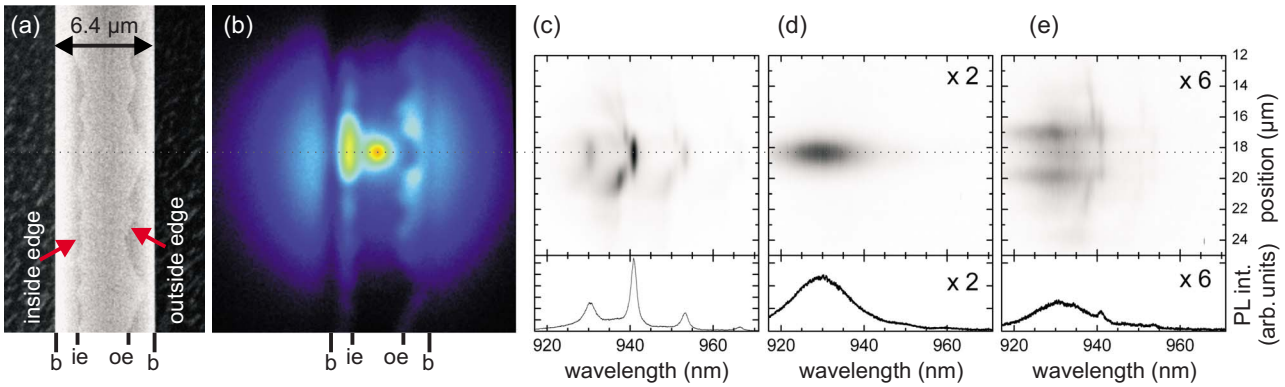

FIG. 3. (Color online) (a) SEM picture of a part of the microtube. Both the inside and outside edges are visible. (b) Undispersed PL image of the sample shown in (a). Both images are equally scaled; the positions of the borders (b), the inside edge (ie), and the outside edge (oe) are marked. [(c)–(e)] Spectrally analyzed PL emission at the (c) inside edge, (d) radial position of the laser spot, and (e) outside edge. In the upper panels, the spatial information along the tube (z) axis is retained. The lower panels show spectra obtained at the z position on the level of the laser spot (marked by the dotted horizontal line). The excitation power density was about 5 kW/cm^2.

Figure 3(a) shows a magnified SEM picture of a part of the investigated self-supporting microtube bridge. As previously mentioned, the tube has rolled up slightly more than two times. For this particular microtube, the small region where the wall consists of three rolled-up strained layers was orientated on top of the tube, just like as that sketched in Fig. 1. Using a rather high acceleration voltage of 20 kV at the SEM, not only the outside edge of the microtube wall but also the inside edge can be resolved. Since the microtube wall in the region between the inside (left) and outside (right) edges consists of three rolled-up layers, it appears slightly brighter in the SEM picture than the material besides this region. We find that applying our preparation technique to the layer system described above, both edges of the microtube tend to randomly fray over some microns instead of forming straight lines. The fraying occurs predominantly along the ⟨110⟩ direction of the crystal, whereas the rolling direction of the microtube is along ⟨100⟩. The spectrum in Fig. 1 proves that optical modes can still develop despite the frayed edges, since it is actually obtained from exactly the microtube shown in Fig. 3(a). By using the grating of the monochromator in zero order as a mirror, we can directly image the microtube on the CCD chip of the detector, as shown in Fig. 3(b). Here, the microtube was excited by the laser, but in the collected signal, the laser stray light was cut off by an edge filter. Therefore, Fig. 3(b) shows an undispersed PL image of the sample. We observe strong emission at the excitation position centrally on the mircotube. We also observe a large corona around this position due to PL emission of the underlying GaAs substrate. The borders of the microtube become apparent by vertical shadows. Furthermore, both the inside and outside edges of the tube are visible in the CCD image. Even though close to the resolution limit, the larger frays especially of the outer edge, which are clearly visible in the SEM picture in (a), can also be identified in (b). Interestingly, we observe a strong enhancement of PL emission near the inside edge of the microtube. Having aligned the microtube axis in the way that its image is parallel to the entrance slit of the spectrometer, we can spectrally analyze the PL light of different radial positions retaining spatial resolution along the tube axis. In Fig. 3(c), the signal along the inside edge is analyzed. The vertical axis gives the spatial position along the tube axis (z direction), the horizontal axis gives the spectral position, the PL intensity is encoded in a gray scale. The lower panel in (c) shows a spectrum obtained at the z position on a level of the laser spot (dotted horizontal line). The sequence of maxima of different wavelengths shows that the light is indeed dominantly emitted out of resonant modes. In Fig. 3(d), the signal emitted underneath the laser spot is analyzed. In contrast to the inner edge, here, only one peak around 930 nm is observed, which is the emission of the QW into leaky modes as already discussed in the context of Fig. 1(a). At last, Fig. 3(e) analyzes the emission at the outside edge. Here, we observe both sequences of resonant modes and leaky modes, but with a much smaller intensity than in (c) or (d). Note that the intensity in (e) is multiplied by a factor of 6 compared to (c). Thus, as a summary of Fig. 3, preferential emission of modes at the inside edge is proven. This result, which is valid for every position along the tube, indicates that the edges of the microtube might be functionalized for a controlled or even directional emission of light.

In order to investigate the influence of the frayed edges on the mode spectrum, we performed micro-PL measurements scanning along the tube (z) axis, which are shown in Fig. 4(b). The graph's horizontal axis gives the wavelength of the detected light, whereas its vertical axis gives the axial position on the microtube which can directly be related to the SEM picture in Fig. 4(a). The PL intensity is encoded in a gray scale where dark means high signal. Note that the gray scale is chosen to be logarithmic in order to better resolve in one and the same graph both intense peaks on a comparatively intense background and small peaks on a weak background. The microtube was scanned in 80 steps over a length of 35 μm [between the two broken horizontal lines in Fig. 4(a)]. In the z direction, the collecting position of the PL light was centered on the excitation spot; in radial direction, we collected over the whole microtube.

For nearly every position on the microtube, we observe three or four optical modes. Their energies are shifting along

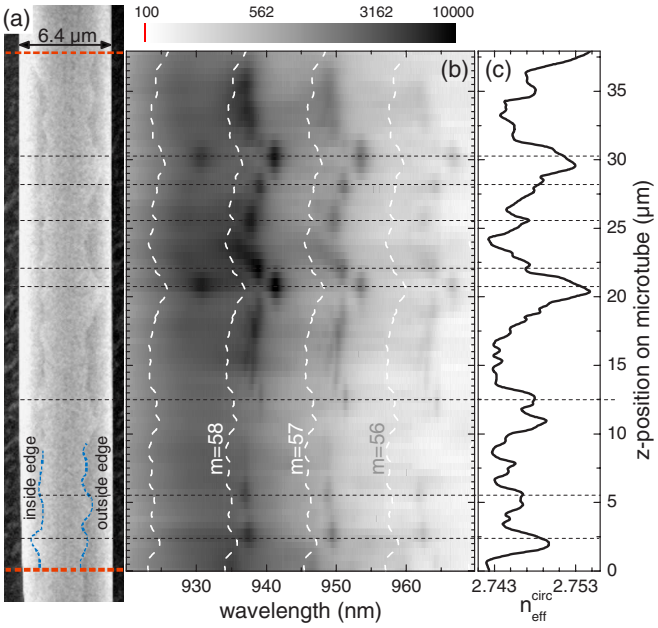

FIG. 4. (Color online) (a) SEM picture of a part of the microtube. Inside and outside edges are marked with broken lines for clarification. The tube wall is thicker between these edges (see sketch in Fig. 1). (b) Scanning micro-PL spectra show three dimensionally confined optical modes (excitation power density of about 4 kW/cm^2). The white broken lines represent calculated mode energies for $m=59$ to 56. (c) Calculated effective refractive index vs position. Horizontal broken lines mark the positions of some pronounced localized modes.

the z direction, but interestingly this shifting is not continuous: The mode energies sometimes seem to be spatially pinned. First, we want to explain the shifting by an expanded model of a closed waveguide. For each position in the z direction, we regard a cross section perpendicular the tube axis as a circular waveguide, having a diameter of $d=6.4$ μm. The waveguide thickness abruptly changes at the edges from 130 to 195 nm. For each region, we translate the thickness in related effective refractive indices $n_{\mathrm{eff}}^{130\ \mathrm{nm}}$ and $n_{\mathrm{eff}}^{195\ \mathrm{nm}}$, respectively.[7] For this calculation, we assumed the average refractive index of the layer system to be $n(E)=0.3225\times E[\mathrm{eV}]+2.982\,32$ by linearly approximating values given in Refs. 11 and 12. From Fig. 4(a), we determine the distance $L^{195\ \mathrm{nm}}(z)$ from the inside to the outside edge on the tube surface by taking into account that the picture is a projection of a curved surface. We can then define an overall effective refractive index for the whole circular waveguide for each z position: $n_{\mathrm{eff}}^{\mathrm{circ}}(z)=n_{\mathrm{eff}}^{195\ \mathrm{nm}}L^{195\ \mathrm{nm}}(z)/(\pi d)+n_{\mathrm{eff}}^{130\ \mathrm{nm}}[1-L^{195\ \mathrm{nm}}(z)/(\pi d)]$. The periodic boundary condition for a resonant mode then reads $n_{\mathrm{eff}}^{\mathrm{circ}}(z)\pi d=m\lambda$, with the vacuum wavelength λ and the azimuthal mode number $m\in\mathbb{N}$. The resonances calculated with this model have azimuthal mode numbers around $m=57$ and are depicted in Fig. 4(b) as bright broken lines. The absolute position of the calculated mth mode strongly depends on the exact dimension of the microtube, whereas the calculated mode spacing fits quite well to the measurements. Deviations can be explained by slightly insufficient approximated refractive index of the layer system, especially because of neglecting absorption inside the QW. As a striking result, the calculation reveals that the overall z dependency of the measured resonant wavelengths is nicely approximated by our model.

In the following, we want to concentrate on the spatially pinned resonances. These resonances can be seen in Fig. 4(b) as isolated dark spots with no significant wavelength shift over 1 μm or more. This implies that these resonances are localized modes, confined also in the z direction along the tube axis. Comparing Figs. 4(a) and 4(b), it seems that some of these localized modes can be attributed to positions on the tube with a broad distance between inside and outside edges. To work out this point in more detail, Fig. 4(c) shows $n_{\mathrm{eff}}^{\mathrm{circ}}(z)$ calculated for $\lambda=940$ nm, which essentially reflects the distance between the edges as a function of the z position. Comparing now (b) and (c), it becomes obvious that optical modes are predominantly localized in regions of local maxima of $n_{\mathrm{eff}}^{\mathrm{circ}}(z)$ representing local maxima of $L^{195\ \mathrm{nm}}(z)$. To better visualize this behavior, all pronounced localized modes are indicated with horizontal lines in Fig. 4(b). Confinement of light along the z direction is achieved by a change of $n_{\mathrm{eff}}^{\mathrm{circ}}(z)$. This important result can be qualitatively explained within the waveguide model. Until now, we implied in our model light having no wave vector component along the tube axis, because, for a perfect infinite microtube, this light would just run away along the tube axis. If we now regard light with a finite but small wave vector component along the axis, this light can experience total internal reflection also in z direction, which leads to a three dimensional confinement. Total internal reflection in this case is quite similar to the situation in a graded-index optical fiber. Our model using an averaged effective refractive index for a circular cross-sectional area of a microtube explains our measured data astonishingly well, despite the fact that this model neglects the abrupt changes of the inside and outside diameters. The experimental data show that it is possible to confine light also along the axis of a microtube ring resonator by a slight change of the wall geometry along the axis. This result opens up new prospects for a controlled three dimensional confinement of light inside a microtube ring resonator by the use of a lithographically controlled variation of the inside and outside edges of the strained layer system before the roll-up process takes place. In this context, we would like to refer to a recent theoretical work by Louyer *et al.* on prolate-shaped dielectric microresonators.[13] We believe that our technique of laterally structuring the edges of a microtube before the roll-up process, which is presented in this paper, might make it possible to fabricate prolate-shaped microtube resonators with similar characteristics as described in Ref. 13.

In summary, we report on a microtube resonator with embedded QWs. We observe optical modes in a quite large energy range, which are partly affected by reabsorption. Scanning micro-PL measurements demonstrate (i) preferential emission of light near the inside edge of the microtube and (ii) confinement of light also in the direction along the tube axis. The confinement is induced by spatial variations of the inside and outside edges of a microtube along its axis and can be approximated in an expanded waveguide model. The

presented results highlight the possibility of both a controlled emission and a controlled three dimensional confinement of light in a microtube by a lithographically controlled definition of the microtube edges.

We gratefully acknowledge financial support of the Deutsche Forschungsgemeinschaft via the SFB 508 "Quantum Materials" and the Graduiertenkolleg 1286 "Functional Metal-Semiconductor Hybrid Systems."

*tkipp@physnet.uni-hamburg.de

[1] K. J. Vahala, Nature (London) **424**, 839 (2003).
[2] G. Khitrova, H. M. Gibbs, M. Kiraz, S. W. Koch, and A. Scherer, Nat. Phys. **2**, 81 (2006).
[3] V. Y. Prinz, V. A. Seleznev, A. K. Gutakovsky, A. V. Chehovskiy, V. V. Preobrazhenskii, M. A. Putyato, and T. A. Gavrilova, Physica E (Amsterdam) **6**, 828 (2000).
[4] O. G. Schmidt and K. Eberl, Nature (London) **410**, 168 (2001).
[5] M. Hosoda, Y. Kishimoto, M. Sato, S. Nashima, K. Kubota, S. Saravanan, P. O. Vaccaro, T. Aida, and N. Ohtani, Appl. Phys. Lett. **83**, 1017 (2003).
[6] S. Mendach, T. Kipp, H. Welsch, C. Heyn, and W. Hansen, Semicond. Sci. Technol. **20**, 402 (2005).
[7] T. Kipp, H. Welsch, C. Strelow, C. Heyn, and D. Heitmann, Phys. Rev. Lett. **96**, 077403 (2006).
[8] S. Mendach, R. Songmuang, S. Kiravittaya, A. Rastelli, M. Benyoucef, and O. G. Schmidt, Appl. Phys. Lett. **88**, 111120 (2006).
[9] M. Hosoda and T. Shigaki, Appl. Phys. Lett. **90**, 181107 (2007).
[10] T. Kipp, K. Petter, C. Heyn, D. Heitmann, and C. Schüller, Appl. Phys. Lett. **84**, 1477 (2004).
[11] T. Takagi, Jpn. J. Appl. Phys. **17**, 1813 (1978).
[12] A. N. Pikhtin and A. D. Yas'kov, Sov. Phys. Semicond. **14**, 389 (1980).
[13] Y. Louyer, D. Meschede, and A. Rauschenbeutel, Phys. Rev. A **72**, 031801(R) (2005).